https://doi.org/10.5194/egusphere-2025-1393
Preprint. Discussion started: 4 April 2025

Spatiotemporal variation of growth-stage specific concurrent climate extremes and their yield impacts for rice in southern China

Ran Sun[1, 4], Tao Ye[1,2,3,4], Yiqing Liu[1, 4], Weihang Liu[1,2,3,4], Shuo Chen[1,2,3,4,5]

[1]State Key Laboratory of Earth Surface Processes and Resource Ecology (ESPRE), Beijing Normal University, Beijing 100875, China
[2]Key Laboratory of Environmental Change and Natural Disasters, Ministry of Education, Beijing Normal University, Beijing 100875, China
[3]Academy of Disaster Reduction and Emergency Management, Ministry of Emergency Management and Ministry of Education, Beijing 100875, China
[4]Faculty of Geographical Science, Beijing Normal University 100875, Beijing, China
[5]Department of Earth, Atmospheric, Planetary Sciences, Purdue University, West Lafayette, IN 47907, USA

Correspondence to: Tao Ye (yetao@bnu.edu.cn)

Abstract. Increasing evidence highlights the disruptive effects of compound climate extremes on global crop yields under climate change. Existing studies predominantly rely on the whole growing-season scale and relative thresholds, and hamper the capture of crop physiological sensitivities and yield responses that vary critically across growth stages. Here, we analyzed the spatiotemporal variations, dominant drivers, and potential impacts on the yields of concurrent heat-drought and chilling-rainy events for single- and late-rice in southern China from 1981 to 2018. Specifically, we carefully distinguished three sensitive growth stages of rice, and used growth-stage-specific physiological thresholds. Temporally, single-rice experienced a significant increase in concurrent heat-drought events, while late-rice experienced a modest rise in chilling-rainy events. Hotspots of concurrent heat-drought events in single-rice systems moved upstream in the Yangtze Basin during the growing season, and the concurrent chilling-rainy events of late-rice were widespread within the planting regions, with a higher incidence in certain areas. These spatial characteristics were primarily driven by spatial differences in phenology rather than the occurrence of extreme events. Path analysis identified heat stress as the primary driver of heat-drought impacts (particularly in jointing-booting and heading-flowering stages), whereas chilling and rainy stress exerted comparable effects for late-rice. Our assessment of compound event impacts and sensitivity to rice yield revealed significant growth-stage-specific differences, with comparable yield losses from both concurrent heat-drought and chilling-rainy events. Single-rice showed the highest sensitivity to heat-drought events during the grain filling stage, whereas the late-rice exhibited greater sensitivity during the heading-flowering stage. The historical yield impact diverged markedly across growth stages, with the largest having occurred in the grain filling stage, particularly for heat-drought events. Our study provided important information on compound agroclimatic extremes, in the context of southern China's rice production system, and the results provide important information for risk management and adaptation strategies under climate change.

https://doi.org/10.5194/egusphere-2025-1393
Preprint. Discussion started: 4 April 2025

1 Introduction

Compound climate extreme events, driven by the interaction of multiple drivers and/or hazards, often have more severe ecological and socioeconomic consequences than single events (Urban et al., 2018; Zscheischler et al., 2020). There is increasing concern regarding the future impacts of compound climate extreme events considering their projected increasing frequency and intensity (IPCC, 2022). Among the multiple potential impacts, agricultural production has received specific attention. The regional threats posed by these extreme events could further lead to global food security issues and the need to develop food system resilience (Chenu et al., 2017; Lobell and Gourdji, 2012; Trnka et al., 2014).

Previous studies have identified increasing trends in compound agroclimatic extremes, mostly in maize and wheat. Globally, analyses using diverse metrics, including growing-season precipitation-temperature anomalies(He et al., 2022), growing-season standardized anomalies of soil moisture and killing-degree-days (Lesk and Anderson, 2021), and Standardized Temperature Index (STI) with multiple drought indicators (i.e., scPDSI, SPI, and SPEI) (Feng et al., 2021), have consistently revealed intensified hot-dry extremes across major crops since 1950, with ~2% annual expansion of maize/wheat areas exposed to such events. Regionally, China's rainfed maize and wheat systems showed similar increasing trends on compound hot-dry days (1980–2015) when assessed by percentiles of daily mean temperature and precipitation (Lu et al., 2018). However, analyses combining temperature indices (heating/freezing degree days) and drought indicators (SPI) or standardized drought-heat indices have revealed limited temporal trends despite the widespread spatial coverage of compound events since 1990 (Li et al., 2022; Wang et al., 2018).

The literature has also investigated the impact of compound agroclimatic extremes on yield, mostly focusing on compound heat and drought events (Lesk et al., 2021). A study on the impact on U.S. soybean yields showed that compound hot and dry summer conditions reduced yields by two standard deviations. This sensitivity is four and three times larger than the sensitivity to hot or dry conditions alone, respectively (Hamed et al., 2021). Another study examined the combined effects of temperature and precipitation on county-level corn and soybean yields in irrigated and rainfed crops in the United States. This shows that combined heat and drought events suppressed rainfed maize and soybean yields (Luan et al., 2021). In addition to concurrent events, the impact of consecutive-dry-and-wet (CDW) extremes on crop yield has also been discussed. Evidence have shown that the risk of yield loss caused by CDW extremes can be twice as high as that from individual wet and dry extremes (Chen and Wang, 2023). Several studies have been conducted to explain crop yield reduction caused by compound heat and drought events from the perspective of temperature–moisture couplings (Lesk et al., 2021).

Despite the growing recognition of compound climate extremes as critical threats to global food security, critical knowledge gaps persist in quantifying their agricultural impacts. First, while concurrent heat-drought events in staple crops have been extensively documented (Rötter et al., 2018), concurrent chilling-rainy events, although equally destructive, remain understudied, particularly in monsoon-dominated agroecosystems (Chen and Wang, 2023). Second, for the analyses of

https://doi.org/10.5194/egusphere-2025-1393
Preprint. Discussion started: 4 April 2025

compound severity, there has been a preference for the use of relative thresholds (e.g., percentiles of indicators) rather than crop-specific physiological thresholds to define extremes. Nevertheless, the use of relative thresholds cannot reflect the crop's biophysical sensitivity to climate extremes, which vary by growth stage and event type (Kern et al., 2018). For example, rice faces different chilling thresholds of ≤ 17 °C at the booting stage and ≤ 20 °C at the grain-filling stages (Zhang et al., 2014). Third, growing-season-scale analyses mask critical sub-seasonal dynamics: extremes during flowering stage disrupt pollen viability and fertilization, whereas grain-filling stages extremes impair sucrose transporters critical for yield formation (Sehgal et al., 2018; Xiong et al., 2016); however these mechanisms remain poorly integrated into impact assessments. Additionally, quantitative analyses of yield losses under compound extreme hobble risk projections are limited.

Rice, as a critical staple crop for a large portion of the global population, deserves particular attention (Yu et al., 2024). Rice production in China includes single-rice in northeast China and in the Yangtze River Basin, and late-rice in southern parts of the country. The climate of these rice cropping systems varies substantially, from sub-tropical to warm temperate, and consequently the crop is exposed to a range of agroclimatic extremes. For single-rice, summer (July to September) is the highest temperature period in southern China and is prone to seasonal drought (Tan et al., 2020). At this time, single-rice in its jointing to flowering and maturity stage is vulnerable to the combined effects of heat and drought. From September to October each year, late-rice in its heading-flowering and grain filling stages is critically vulnerable to low temperatures, strong winds, and persistent rainy weather (Guo et al., 2020). These climate extremes compounded together are commonly referred to as "chilling-dew wind" and "continuous rain" events (Xie et al., 2016; Zhang et al., 2021). Climate change has driven more frequent and intensive extreme events for rice cultivation (He et al., 2022; Yu et al., 2024). The 2022 summer compound hot-dry events in the Yangtze River Basin once induced considerable worry about the rice-based autumn grain production in southern China (Fu et al., 2024). Therefore, focusing on the compound climate extremes related to rice production in China could help add new wisdom about compound agroclimatic extremes to those reported about other staple crops.

This study aims to explore the spatiotemporal variations of concurrent compound extremes (CCEs) for single- and late-rice in southern China during the period 1981−2018, identify their underlying drivers, and assess their yield impact. Here, concurrent events refer to cases in which multiple types of extremes occur in the same growth stage. Unlike previous studies, we carefully distinguished CCEs by specifying the growth-stage physiological thresholds. We divided the rice-growing season into three critical stages: the jointing-booting stage (#1), heading-flowering stage (#2), and grain filling stage (#3). We considered four types of climate extremes that could substantially affect rice yield: heat (H), drought (D), chilling (C) and rainy (R). Correspondingly, we considered concurrent heat-drought events for single-rice, and concurrent chilling-rainy events for late-rice. Our main questions are as follows: (1) How did the concurrent heat-drought and chilling-rainy events change temporally and spatially for rice in southern China during 1981-2018? (2) How was the temporal change in the severity of compound events driven by that of individual events? (3) To what extent do these concurrent events cause yield losses? (4) How did the answers to the above question differ by the rice growth stage?

https://doi.org/10.5194/egusphere-2025-1393
Preprint. Discussion started: 4 April 2025

2 Materials and Methods

2.1 Study area

Our study area covers the major rice-growing areas in southern China (Fig. 1). Local rice-growing systems include typical late-rice in the southeast and single-season rice (hereafter "single-rice") in the Yangtze River basin and southwestern China. Late-rice generally grows from July to November and is subjected to extremely low temperatures and continuous rain from September to October. Single-rice generally grows from June to November. Its heading-flowering stages overlap with the hottest season and are prone to drought owing to the hilly terrain of southern China (Tan et al., 2020). To best present the complicated temporal structure of climate extremes, both single- and late-rice were considered in our analyses.

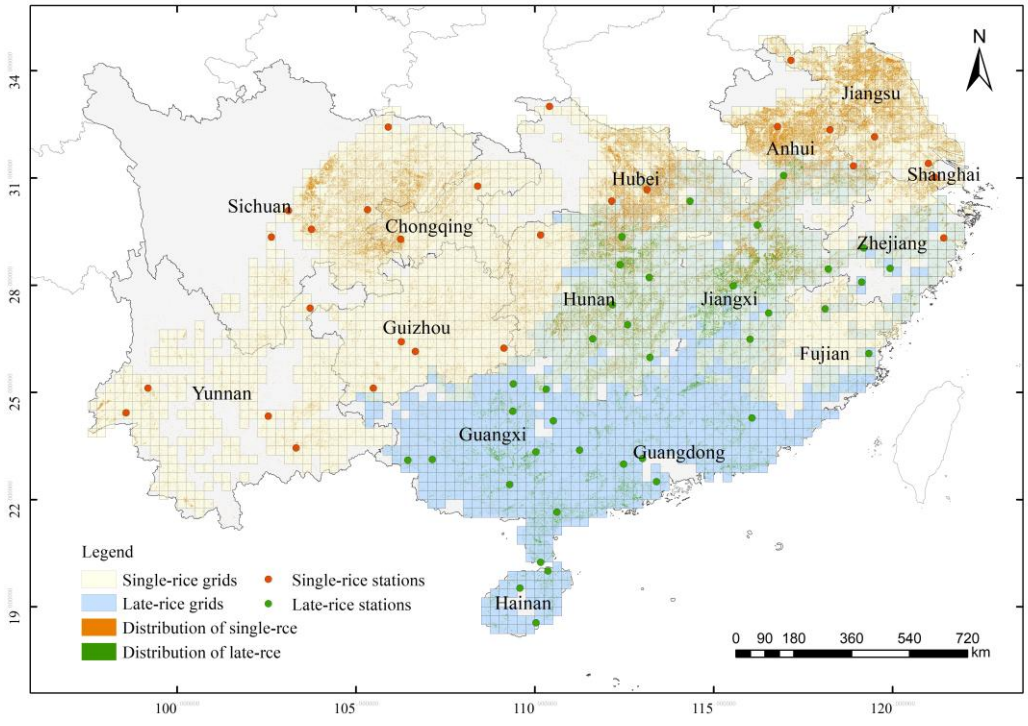

Figure 1. Raster samples of single-rice and late-rice growing areas. Yellow grids indicate areas where single-rice is grown and blue grids indicate areas where late-rice is grown.

2.2 Data

A gridded daily dataset containing daily mean temperature and precipitation was obtained from the CN05.1 dataset prepared by the Institute of Atmospheric Physics, Chinese Academy of Science (Wu and Gao, 2013). The CN05.1 is a gridded daily dataset based on interpolation from over 2400 observation stations in China, with spatial resolution of 0.25° latitude and 0.25° longitude. It is regarded as the best choice for gridded climate forcing data in mainland China and has been widely used and

https://doi.org/10.5194/egusphere-2025-1393
Preprint. Discussion started: 4 April 2025

tested in previous studies (Li et al., 2022; Zhu and Yang, 2020). The 0.25° gridded daily 0-10 cm soil moisture data were obtained from the VIC-CN05.1 surface hydrology dataset (Miao and Wang, 2020). The dataset was simulated by the latest variable infiltration capacity (VIC) model and driven by pure station-based atmospheric forcings and high-resolution soil parameters based on field surveys. The modeled 0-10 cm soil moisture anomalies were highly correlated with in situ measurements (438 stations) during 2003–2016, with a mean R = 0.80.

Two versions of rice phenology dataset were used to derive gridded rice phenological dates. Rice phenological dates recorded by agrometeorological stations from 1981 to 2014 were obtained from the China Meteorological Administration (CMA, http://data.cma.cn). This dataset is considered the best quality crop phenology observation station dataset in China and has gained widespread usage (Chen et al., 2021; Liu et al., 2023; Zhang et al., 2022a). Each station meticulously documents the rice cropping type (single-rice or late-rice) and the corresponding dates for every phenological event during the rice-growing season following the specifications for agrometeorological observation—Rice (QX/T 468–2018). Rigorous checks and validation during the data preparation process resulted in the production of extremely accurate data on rice phenology, with an accuracy rate exceeding 95%. Records that exceeded twice the standard deviation were rejected to ensure the data quality (Zhao et al., 2016). Rice phenology data in 1-km grids covering period of 2000-2019 were obtained from the ChinaCropPhen1km dataset (Luo et al., 2020). This data were derived based on Global Land Surface Satellite (GLASS) leaf area index (LAI) products. This dataset is superior to the previous one due to its spatially gridded format, but does not offer information before 2000. Both datasets were later fused to derive annual phenological dates from all rice-growing grids.

The annual spatial distribution data of single and late rice were obtained from a high-resolution distribution dataset of single-rice (Shen et al., 2023) and late-rice (Pan et al., 2021). The dataset provided a 10-m gridded distribution of single rice for 21 provinces in China and that of late rice for nine provinces in Southern China. The two datasets used a method that combined optical and synthetic aperture radar images based on the time-weighted dynamic time warping method. For single-rice, the data achieved an average overall accuracy of 85.23% across 21 provincial regions, based on 108,195 samples, with a mean R^2 value of 0.83 when compared to county-level statistical planting areas over three years. For late-rice, the identification accuracy reached 90.46% based on 145,210 survey samples. We took the data for 2020 as the southern China rice-growing area mask.

Historical gridded rice yield data were obtained from the AsiaRiceYield4km dataset (Wu et al., 2023) covering 1995 to 2015. The AsiaRiceYield4km dataset was generated by integrating multisource predictors into machine learning models, using inverse probability weighting to select the optimal model. It achieved high accuracy for seasonal rice yield estimation, with R^2 value of 0.88 and 0.91for single and late-rice, and significantly outperformed existing models. Thus far, the dataset provides the longest time series covering all rice cultivation areas in China.

Owing to the difference in the spatial resolution of the above datasets, we harmonized those data to one base grid for later analyses. We used 0.25°×0.25° grids of the CN05.1 dataset as the base. Rice-growing area masks for single rice and late rice

https://doi.org/10.5194/egusphere-2025-1393
Preprint. Discussion started: 4 April 2025

were then applied to the base grid map to mask valid rice-growing grids. As one single 0.25°×0.25° climate grid covered many 10-m rice pixels, we kept climate grids with rice pixels ≥5% of the area of each climate grid. The final base map contained 2262 0.25°×0.25° grids for single-rice and 1383 0.25°×0.25° grids for late-rice (Fig. A1). For each grid, rice phenological dates were interpolated from station-observed dates using the co-kriging method with Gaussian function, and the gridded phenology information from the ChinaCropPhen1km dataset as a covariate. Our interpolation effectively captured spatial variability characteristics and compensated for the sparse coverage of station observations in many areas. We also adjusted the resolution of AsiaRiceYield4km to the base grid using bilinear interpolation.

2.3 Compound types and thresholds for concurrent events

Three stages of rice growth that were most susceptible to extreme weather stress were considered in this study: the jointing-booting stage (#1), the heading-flowering stage (#2) and the grain filling stage (#3). The jointing-booting stage refers to the period from jointing to the day before heading. The heading-flowering stage refers to the period from heading to flowering and generally lasts for 10 days. The grain filling stage refers to the period from the 11th day after heading to maturity. The exact dates of the different stages were obtained from phenological records for each year and station.

We considered four types of climate extremes that could substantially affect rice yields: drought, heat, chilling and rainy. To determine the thresholds, we referred to national and provincial standards for each stress. Our preliminary analysis showed that strictly adhering to these official thresholds led to a small sample size for a valid statistical analysis. Consequently, after a thorough literature review, we relaxed the thresholds of duration but reserved those for temperature/moisture. Finally, we specified thresholds for each climate extreme by growth-stage (Table 1), which were applied to daily climate data to screen the historical occurrence of these events.

Table 1 The thresholds of each type of extreme event.

Rice type	**Growth stage**	**Climate extremes**	**Indicator & threshold: daily mean temperature *(T/℃)*, daily total precipitation *(PRE/mm)*, soil moisture *(SM/%)***	
Single-rice	Jointing-booting (#1) Heading-flowering (#2) Grain filling (#3)	Heat	T ≥ 33 ℃	≥ 1 successive day
		Drought	SM ≤ 75 %	≥ 10 successive days
Late-rice	Heading-flowering (#2)	Chilling	T ≤ 20 ℃	≥ 1 successive day
		Rainy	P ≥ 25 mm	≥ 1 successive day
	Grain filling (#3)	Chilling	T ≤ 17 ℃	≥ 1 successive day
		Rainy	P ≥ 25 mm	≥ 1 successive day

Note: The above thresholds are referenced from: <NY/T 2915-2016>, Identification and classification of heat injury of rice; <NY/T 3043-2016>, Code of practice for field investigations and classification of rice seasonal drought stressess in southern-

https://doi.org/10.5194/egusphere-2025-1393
Preprint. Discussion started: 4 April 2025

China; <NY/T 2285-2012>, Technical specification of field investigations and the grading of chilling damage to rice and; <DB5101/T 125-2021>, Indica rice weather stress level-continuous rain. NY/T is the *Agricultural Information Resource Classification and Coding Specification* in China. DB5101/T is the *Local Standard of Chengdu, Sichuan Province*. Thresholds for duration were relaxed from original standards to ensure adequate samples for later analyses.

For compound climate extremes, we exclusively considered the case in which two types of stress occurred in the same growth stage, that is, simultaneous exposure to heat and drought during the jointing-booting stage of single-rice. This structure followed the topological structures suggested by Zscheischler (Zscheischler et al., 2020) and is hereafter referred to as concurrent climate extremes (CCEs). Correspondingly, we have three CCEs for late rice, namely, concurrent heat-drought events in the jointing-booting stage (H1D1), heading-flowering stage (H2D2), and grain filling stage (H3D3). The same rule of naming was also applied to single rice, which has two CCEs: C2R2 and C3R3.

2.4 Severity of individual and compound climate extremes

Here, severity (Haqiqi et al., 2021) was used to measure the stress imposed by individual extreme event. It was defined as the cumulative deviation from the threshold value of each stress. Following the concept, heat stress (*H*) severity $S_{H,g,t}$ at a given growth stage (*g*) in a given year (*t*) that meets the condition can be computed by the cumulative deviation of mean daily temperature (*T*) above its threshold (T_{base}) for all the days (*i*) within this stage. We used 33°C as the base temperature (Table 1) in Eq. (1).

$$S_{H,g,t} = \sum_{i=1}^{n} |T_i - T_{base}| \ (T_i \geq T_{base}) \quad (1)$$

Similarly, chilling stress severity $S_{C,g,t}$ can be computed by the cumulative deviation of daily mean temperature (*T*) below its threshold (T_{base}), for which we used 20 °C for heading-flowering stage and 17 °C for grain filling stage for one or more consecutive days in Eq. (2). Drought stress severity $S_{D,g,t}$ can be computed by the cumulative deviation of soil moisture (SM_i) $\leqslant$75 % (SM_{base}) for ten or more consecutive days in Eq. (3). Rainy stress severity $S_{R,g,t}$ can be computed by the cumulative deviation of daily total precipitation (PRE) $\geq$ 25 mm (PRE_{base}) for one or more consecutive days in Eq. (4).

$$S_{C,g,t} = S_T = \sum_{i=1}^{n} |T_i - T_{base}| \ (T_i \leq T_{base}) \quad (2)$$

$$S_{D,g,t} = S_{SM} = \sum_{i=1}^{n} |SM_i - SM_{base}| \ (SM_i \leq SM_{base}) \quad (3)$$

$$S_{R,g,t} = S_{PRE} = \sum_{i=1}^{n} |PRE_i - PRE_{base}| \ (PRE_i \geq PRE_{base}) \quad (4)$$

For each grid, severity of heat, drought, chilling, and rainy stress were computed by growth stage by using above equations.

https://doi.org/10.5194/egusphere-2025-1393
Preprint. Discussion started: 4 April 2025

To provide a metric for the severity of compound events, copulas were used to fit marginal distributions of CCEs specified in Table 1 to derive compound severity. Copulas have been widely used in modeling compound climate extremes by constructing bivariate models (Li et al., 2021; Tavakol et al., 2020). It provides distinct advantages for multivariate analysis, including the ability to separately model marginal distributions and joint dependence, a mathematically feasible formulation, and the flexibility to select various marginal distributions (Sadegh et al., 2018; Salvadori et al., 2016; Vandenberghe et al., 2010). Specifically, the dependence structure between univariate indices (temperature and precipitation) was modeled using copula theory to fit a joint distribution of these variables (Madadgar et al., 2016; Mazdiyasni et al., 2019). The copula C for two random variables X and Y can be represented as follows:

$$P(X \leq x, Y \leq y) = C[F(X), G(Y)] = C(u, v) \quad (5)$$

where $u = F(X)$ and $v = G(Y)$ are marginal distributions of the random variables X and Y, respectively. X and Y represent the univariate indices (severity) of climate extremes for the given growth stage in Table 2. For instance, the joint distribution of concurrent heat-drought event across stages #1 can be fitted by using the severity of heat stress S_H for stage #1 of all grids and all years together with that of the drought stress S_D of stage #1. After fitting the best Copulas, joint cumulative distribution functions for non-exceedance probabilities for all CCEs were derived. For each grid and each year, the two-dimensional severity could then be transformed into an exceedance probability by exceedance probability conversion. It was actually a probability conditioning on the occurrence of specific compound extremes. To reveal the total probability of specific events, we converted the conditional probability back to the total probability, by using $P(A) = P(A|B) \times P(B)$:

$$P_{S_{H1}S_{D1}} = P(S_{H1} \geq x, S_{D1} \geq y | x > 0, y > 0) \cdot P(x > 0, y > 0) = [1 - u - v + C_{H1D1}(u, v)] \cdot \frac{n(x>0, y>0)}{N} \quad (6)$$

The total probability $P_{S_{H1}S_{D2}}$ is then the joint exceedance probability of both severities, and can be regarded as a measure of the severity of compound extremes, where larger absolute P values denote more severe conditions. A more convenient expression of the CS (compound severity) is to express the total probability P as a standardized z-score by using the inverse transformation:

$$CS_{H1D1} = \varphi^{-1}[P_{S_{H1}S_{D1}}] \quad (7)$$

where φ^{-1} is the inverse transformation function of the standard normal distribution. Larger CS values denote more severe conditions.

To identify suitable models when fitting those copulas, we first conduct goodness-of-fit tests at a 0.05 significance level (Salvadori et al., 2016). The best-fitting admissible model is then determined using the Bayesian Information Criterion (BIC) (Ribeiro et al., 2020). Models that cannot be rejected, based on p-values at the 0.05 significance threshold, are considered for

https://doi.org/10.5194/egusphere-2025-1393
Preprint. Discussion started: 4 April 2025

final selection (Li et al., 2022; Sadegh et al., 2018). In this study, the Clayton copula was selected to construct the compound climate extremes. For the spatial distribution of severity, the average severity across all years with occurrence was used.

2.5 Contribution of temporal changes of Individual stress to compound events

We attempted to understand how the temporal changes in individual stress were attributed to compound climate extremes. Specifically, we attempted to determine how the changes in compound severity (CS) of a specific CCE are related to the corresponding heat/chilling stress severity and drought/rainy stress severity changes over time. Because there can be strong interactions between temperature and moisture, path analysis was conducted. A path analysis decomposes the interaction between the dependent and independent variables (correlation coefficients) into direct (direct path coefficients) and indirect (indirect path coefficients) based on a multiple linear regression, without requiring the variables to be independent of each other (Zhang et al., 2022b). It has been widely applied to estimate the magnitude and significance of hypothesized causal connections between dependent and independent variables when the effects of the variables are confounded (Zhang et al., 2022b, c; Yan et al., 2022).

We separated the system of correlations between the dependent variable and two corresponding independent variables to obtain the path coefficients. Taking single-rice as an example, the path coefficient of heat stress severity (S_H) to compound severity (CS) $R_{S_H,CS}$, which was also the Pearson correlation coefficient between S_H and CS, could be decomposed into direct and indirect effects by:

$$R_{S_H,CS} = P_{S_H,CS} + r_{S_H,S_D} P_{S_D,CS} \quad (8)$$

where, $P_{S_H,CS}$ is the direct path coefficient of S_H on CS, and r_{S_H,S_D} is the Pearson correlation coefficient between the two independent variables, S_H and S_D. Thus, $r_{S_H,S_D} P_{S_D,CS}$ is the indirect path coefficient of drought stress severity on CS. $P_{S_H,CS}$ and $P_{S_D,CS}$ are two standardized linear regression coefficients obtained by regressing CS on S_H and S_D. An *F*-test is conducted to test the statistical significance of the results, and the results of the path analysis were statistically significant when the *p*-value was < 0.05.

Based on the direct and indirect path coefficients, and the independent variables' relative effect on the dependent variable, the determination coefficient (DC) could be derived. The DC for each climate variable is $DC_i = P_i^2$, where $i = S_H, S_D, S_C$ or S_R. For the contribution from the cooperative interaction between two climate variables, the co-determination coefficient is then $DC_{co} = 2P_i r_{ij} P_j$, where $i, j = S_H, S_D, S_C$ or S_R. DC_{co} can indicate the extent to which the interaction of two independent variables affected the compound extremes. The total coefficient of determination (DC_{total}) can be obtained by summing the direct coefficients of determination and the coefficients of co-determination of all independent variables, which was used to indicate the magnitude of the joint explanatory power of individual stress.

https://doi.org/10.5194/egusphere-2025-1393
Preprint. Discussion started: 4 April 2025

2.6 Yield Impact Assessment

The yield impact of CCEs was evaluated using the relationship between the yield anomaly and its corresponding compound severities. Yield anomalies were computed following the methodology outlined by Wang (Holly Wang & Zhang, 2003), in which historical yield trends were fitted first and subtracted from the time series to obtain anomalies. Yield trends were derived by fitting a log-linear regression model. The ordinary least squares method was then applied to fit the model directly to the yield-time series of each grid, enabling us to derive the detrended values for subsequent analysis (Ye et al., 2015). Specifically, the yield Y_t at time t was modeled as:

$$\log(Y_t) = \beta_0 + \beta_1 t + \epsilon_t \quad (9)$$

The detrended yield $Y_{d,t}$ can be calculated as:

$$Y_{d,t} = Y_t - \widehat{Y_t} \quad (10)$$

Where $\widehat{Y_t}$ is the predicted value obtained from the linear regression.

Standardization can be achieved by converting the detrended data into z-scores:

$$YA_t = \frac{Y_{d,t} - \mu}{\sigma} \quad (11)$$

Where YA_t is the standardized yield anomaly. $\mu = \frac{1}{n}\sum_{i=1}^{n} Y_{d,t}$ is the mean of the detrended yield, $\sigma = \sqrt{\frac{1}{n-1}\sum_{i=1}^{n}(Y_{d,t} - \mu)^2}$ and $n - 1$ is used instead of n to provide an unbiased estimate of the population standard deviation.

3 Results

3.1 Temporal changes of compound climate extremes

Using growth-stage-specific thresholds, we quantified compound severity (CS) for each concurrent event across three critical rice stages: jointing-booting (H1D1), heading-flowering (H2D2/C2R2), and grain filling (H3D3/C3R3). We aggregated the grid-level severity into the annual average CS to show the overall temporal changes in compound events (Fig. 2b and 2d). We also plotted the kernel density estimate (KDE) of the annual CS (Fig. 2a and 2c). Higher KDE values at specific time intervals denote clusters of events, whereas lower values suggest sporadic occurrence. For the concurrent heat-drought events of single-rice, the annual CS (Fig. 2b) displayed an increasing trend with a rate of approximately 0.12 per decade, which was statistically significant. H1D1 events, which first appeared in 1981, exhibited clustered occurrences with abrupt KDE peaks around 2003 and 2010. H2D2 events emerged after 1992 but showed sharp KDE increases after 2010, suggesting a shift toward higher

https://doi.org/10.5194/egusphere-2025-1393
Preprint. Discussion started: 4 April 2025

frequency in the recent decade. Unlike the first two events, H3D3 appeared the latest (1998), with a KDE peak between 2005 and 2010, followed by a slow decline after 2010.

Concurrent chilling-rainy events were frequent throughout the historical period (Fig. 2c and 2d). There was only a weak upward trend along the time series, which was not significant. The occurrence of concurrent chilling-rainy events for both stages was less frequent around 2005 (from 2003 to 2007) and peaked around 1981-2000, and 2017.

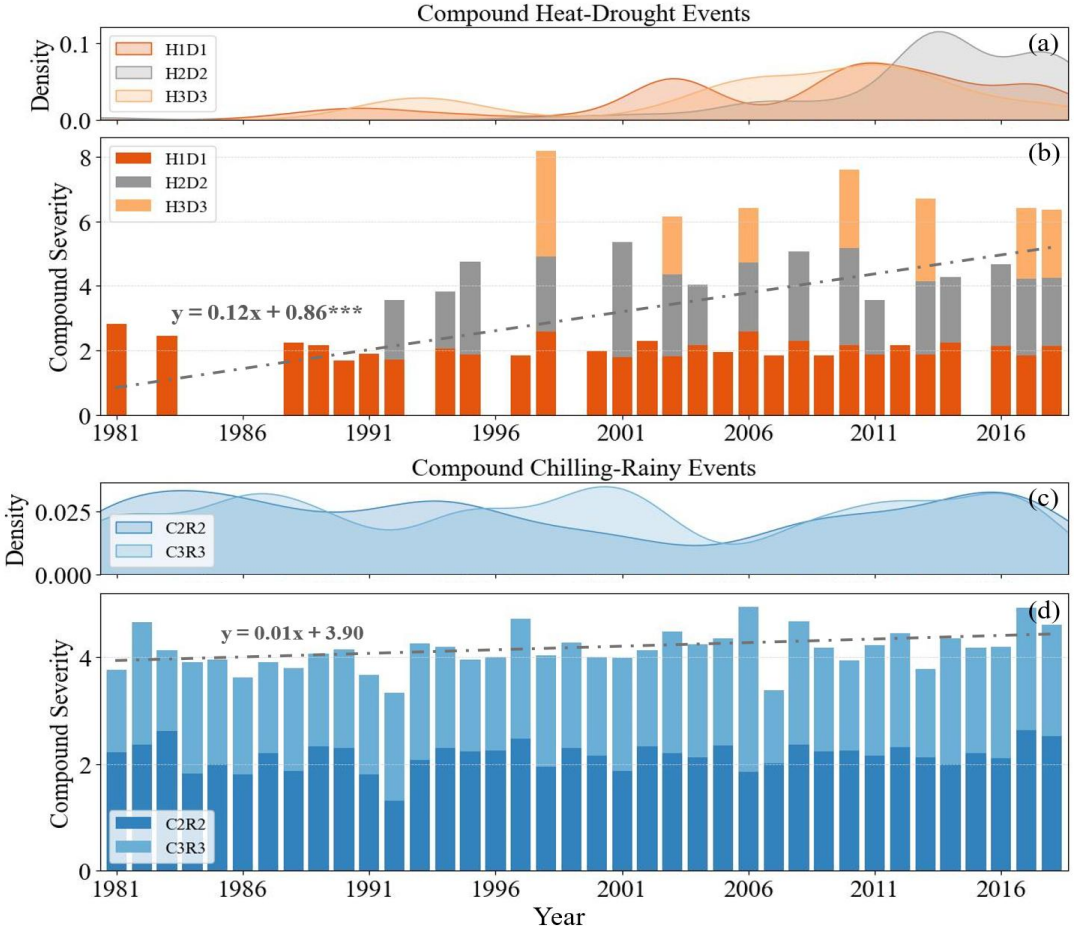

Figure 2. Absolute annual compound severity (b, d) and the kernel density estimate (KDE) (a, c) of concurrent compound events (CCEs) for single- and late-rice during the period of 1981−2018. *** indicates significant at the 0.001 Significance level.

https://doi.org/10.5194/egusphere-2025-1393
Preprint. Discussion started: 4 April 2025

3.2 Spatial distribution of compound climate extremes

We averaged the annual compound severity for each type of CCEs in each grid to map the spatial hotspots (Fig. 3). The patterns were clear and contrasting. The average compound severity for concurrent heat-drought events covered a limited growing area, whereas that for chilling-rainy events was widespread.

285 Hotspots of high-compound severity grids for concurrent heat-drought events differed largely according to growth stage (Fig. 3a-c). The hotspots shifted gradually from the coast (H1D1) to inland China (H3D3) with rice growth. H1D1 was mostly concentrated in the lower reaches of the Yangtze River (East China region), while H3D3 was concentrated in the eastern part of the Sichuan-Chongqing area. H2D2 showed a clustered occurrence in central Anhui, eastern Hunan, and eastern Sichuan.

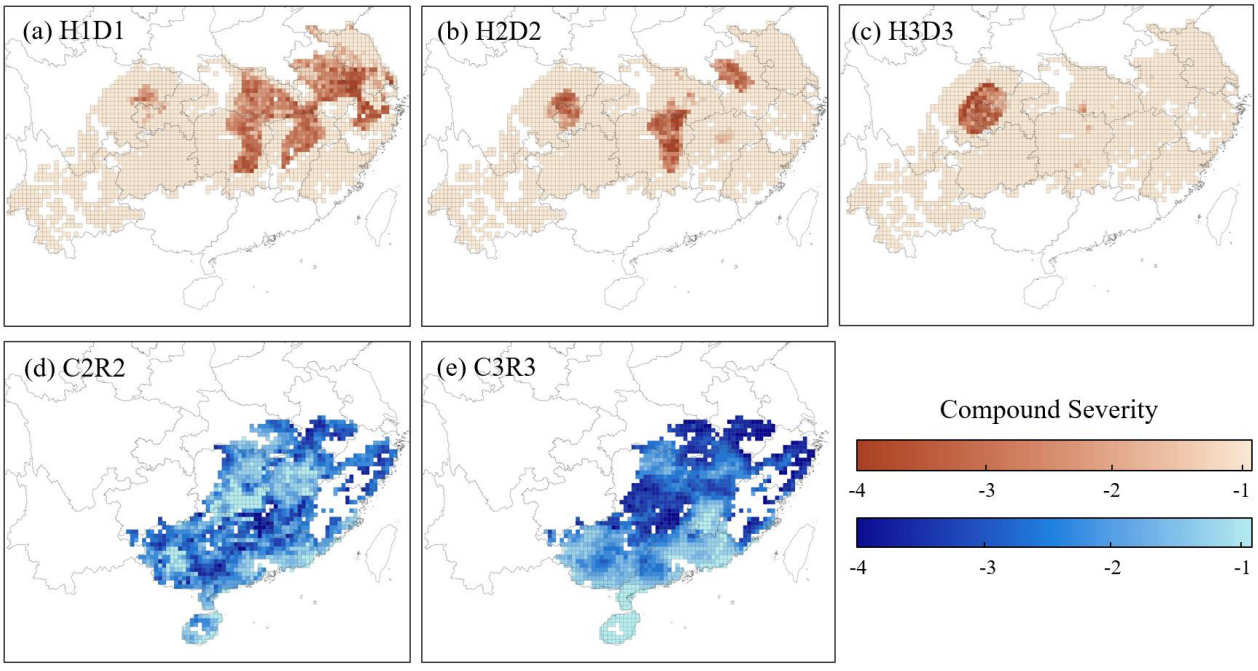

290 **Figure 3. Spatial distribution of the concurrent heat-drought events of single-rice (a-c) and the concurrent chilling-rainy events of late-rice (d, e) for the period of 1981−2018.** The shading indicates the compound severity for each compound event.

Unlike heat-drought events, concurrent chilling-rainy events were widespread within the planting regions, with a higher incidence in certain areas (Fig. 3d and 3e). Hotspots of C2R2 were mostly concentrated in the southern parts of the study area,
295 hilly regions to the south of Hunan and Jiangxi, and eastern Guangxi. The hotspots moved northward in C3R3, reaching the northeastern part of the study area, occurring in Hubei, Anhui, Zhejiang, and hilly regions in southern Hunan province where the altitude is relatively high.

https://doi.org/10.5194/egusphere-2025-1393
Preprint. Discussion started: 4 April 2025

3.3 Effects of individual stress severity on concurrent climate extremes

We took the path coefficient as the relative sensitivity of CS (compound severity) to S_H and S_D for single-rice, S_C and S_R for late-rice. For three types of the concurrent heat-drought events, the direct path coefficient for heat stress severity ($P_{S_H,CS}$) and drought stress severity ($P_{S_D,CS}$) were both positive (Fig. 4a), indicating that the changes in the severities of heat and drought stress both contributed to increasing the compound severity. The contribution of S_H was much larger than S_D in stage#1, but slightly smaller in stage#3. Considering that the distribution of spatial hotspots for concurrent heat-drought events varied markedly across three growth stages (Fig. 3a-3c), the pattern also suggests the regional difference of relative contribution. In the lower-reaches of the Yangtze River Basin, heat stress was a greater determinant of concurrent heat-drought events than the drought stress, while in the eastern Sichuan Basin, the influence of drought stress exceeded slightly the influence of heat stress.

For single-rice, the total determination coefficient, DC_{total}, which indicates the total effect of the two independent variables on the dependent variable, was similar across concurrent heat-drought events (median around 0.9) (Fig. 4c). The single-factor determination coefficients ($DC_{S_H,CS}$ and $DC_{S_D,CS}$) indicated that the severity of heat stress affected the change of concurrent climate extremes to a greater extent than the severity of drought stress in H1D1 and H2D2, with a similar pattern observed for the path coefficients ($P_{S_H,CS}$, $P_{S_D,CS}$). The median DC_{co} was around 0.3, which indicated that the two variables are not independent and positively correlated. It is worth noting that the median of DC_{co} is higher than the median of $DC_{S_D,CS}$ in H1D1 and H2D2, which may result from the dominant effect from heat stress on concurrent heat-drought events in jointing-booting stage (stage #1) and heading-flowering stage (stage #2).

The pattern of the effects of chilling and rainy stress severity on concurrent chilling-rainy events for late-rice was very different to that of heat-drought events (Fig. 4b). Both chilling and rainy stress severity had a strong direct effect on the changes in climate extremes, with chilling having a slightly larger effect in C2R2 and rainy had a slightly larger effect on C3R3. This pattern was also supported by the DCs of individual variables ($DC_{S_C,CS}$ and $DC_{S_R,CS}$) (Fig. 4d). DC_{co} was almost 0 for both growth stages (Fig. 4d), due to the very small indirect coefficient, indicating that there was little correlation between the two stresses in concurrent chilling-rainy events. That means the interactive effects of temperature and moisture had quite small influence on the changes observed in concurrent chilling-rainy events for late-rice.

https://doi.org/10.5194/egusphere-2025-1393
Preprint. Discussion started: 4 April 2025

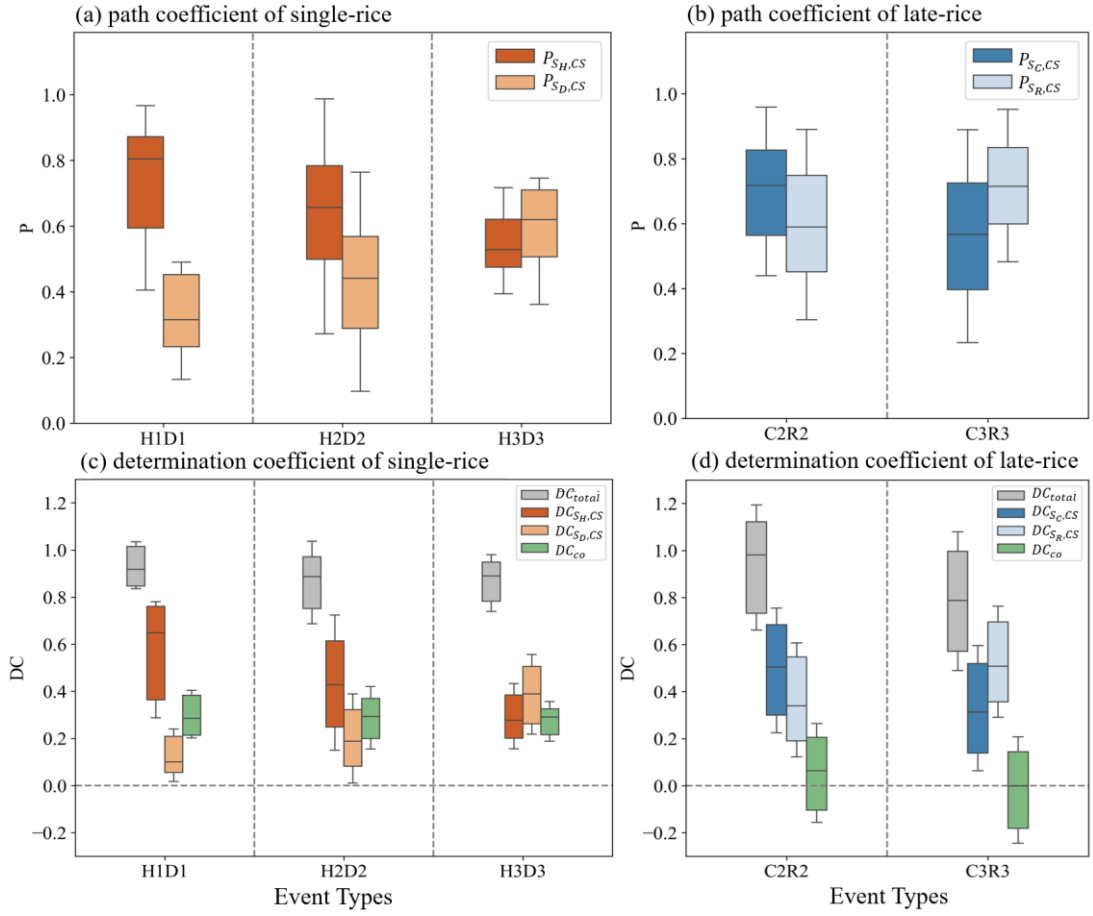

Figure 4. **Boxplot of the path analysis of climate factors on the duration of CCEs for the period of 1981−2018.** *F*-test results that were statistically significant at the 0.01 significance level of were retained in the figure.

3.4 Rice yield impact of compound events

Our yield impact analyses found significantly different historical average yield losses and yield sensitivities across growth stages for both types of CCEs. For concurrent heat-drought events, the average yield loss was the highest in the grain filling stage (H3D3), which was slightly greater than one standard deviation (Fig. 5f). This phenomenon was determined by a combination of the actual compound severity of each event during the historical period, number of years, and size of the region of occurrence.

https://doi.org/10.5194/egusphere-2025-1393
Preprint. Discussion started: 4 April 2025

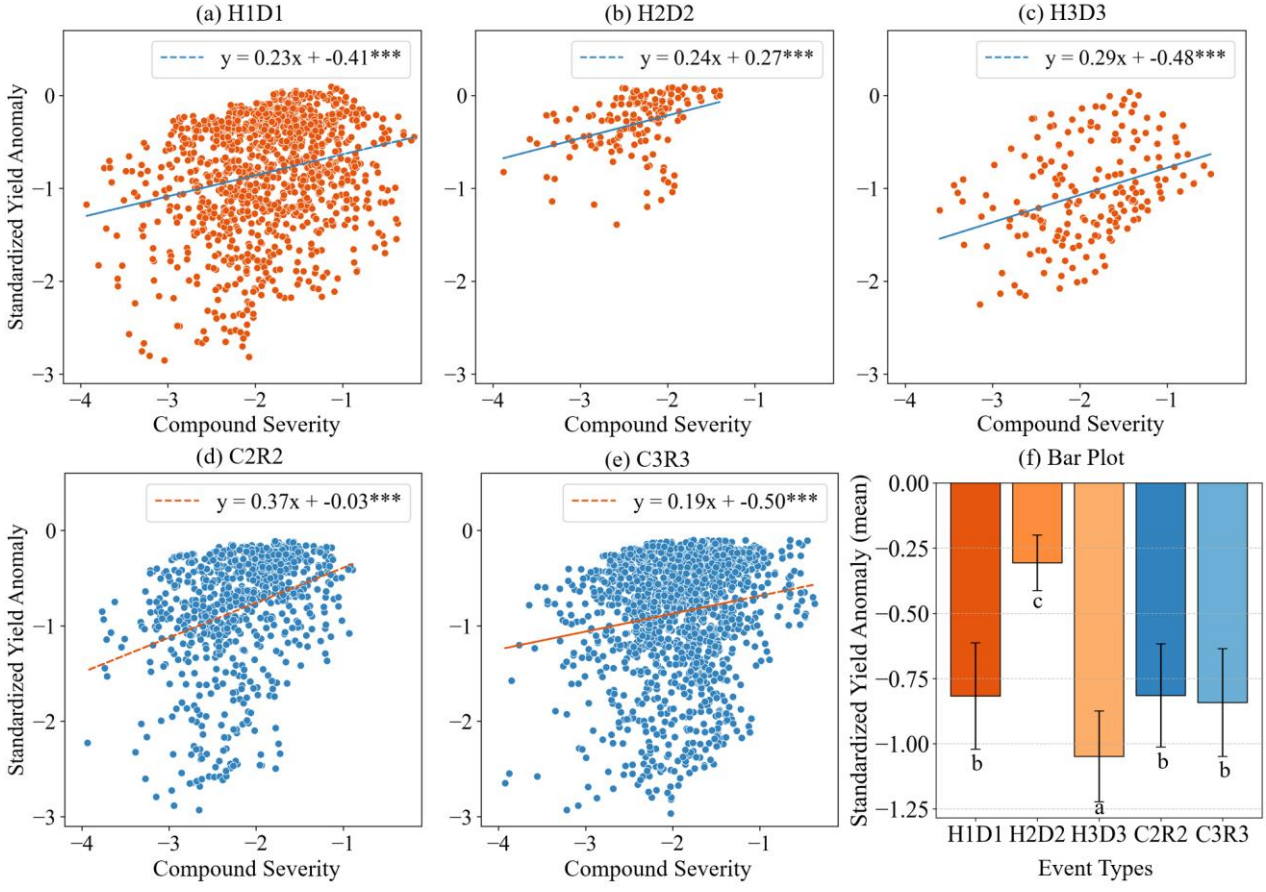

Figure 5. **The compound severity of rice climate extremes versus standardized yield anomaly (a-e) and the bar plot of standardized yield anomaly (f) during the period of 1995−2015.** The symbol * indicates that *F*-test results were significant at the 10% significance level.

We also examined rice yield sensitivity to concurrent events using the scatter plot of the standardized yield anomaly versus compound severity (Fig. 5a-e). A positive correlation was observed between compound severity and yield reduction, which was significant for all event types and growth stages. For single-rice, yield was more sensitive in the grain filling stage (#3) to concurrent heat-drought events, with a linear regression coefficient of 0.29, significant at the 0.05 significance level (Fig. 5c). This indicated that in response to every one standard deviation increase in the compound severity, a single rice yield would drop by 0.29 standard deviation. The sensitivity was slightly smaller in the heading-flowering stage (Fig. 5b) and the smallest in the jointing-booting stage (Fig. 5a), but both were significant. For late-rice, yield was more sensitive in the heading-flowering stage than in the grain filling stage, with a greater slope coefficient of 0.37 than 0.19, both of which were significant (Fig. 5d and 5e).

https://doi.org/10.5194/egusphere-2025-1393
Preprint. Discussion started: 4 April 2025

4 Discussion

4.1 Divergent spatial distribution patterns yet increasing temporal trends of concurrent events for rice

We revealed the spatiotemporal variation of concurrent compound extremes (CCEs) for single-and late-rice in southern China, using growth-stage-specific physiological thresholds for temperature and moisture (either soil moisture or precipitation). This approach minimizes uncertainties inherent in applying uniform thresholds across the entire growing season. For example, the spatial shifts in the hotspots of concurrent heat-drought events of single-rice would have not been identified if we conducted evaluations over the entire growing-season. For the chilling stress to late-rice, the different effects of extremes at the heading-flowering and grain-filling stages would not have been distinguishable if only one single temperature threshold was used to screen the whole growing-season. The consideration of a growth-stage-specific type-threshold enabled us to distinguish the different spatial and temporal characteristics of CCEs in different stages for single-rice and late-rice.

Temporally, we found a statistically significant increasing trend in the compound severity of concurrent heat-drought events, in southern China. The concurrent chilling-rainy events for late-rice had a weak increasing trend, which was insignificant. The result was consistent with the increasing frequency of concurrent heat-drought events reported in previous studies. For example, increasing trends for concurrent heat-drought events in the main crop production areas since 1980 have also been reported by He (He et al., 2022), Zhang (Zhang et al., 2022c) and Lu (Lu et al., 2018). For chilling-rainy events in late-rice, (Liu et al., 2013) also reported that the frequency of chilling events in rice during the period 2001–2011 was higher than that in 1990–2000. They suggested that despite the increase in mean climatic temperatures, the occurrence of chilling events in rice did not decrease, but instead showed a gradually increasing trend. This pattern was also consistent with our findings.

Spatially, we found that concurrent heat-drought events occurred only in specific regions in each of the three growth stages of single-rice, and coincided with the occurrence of heat stress in each growth-stage (Fig. A1). These spatial differences could mainly be attributed to regional differences in rice phenology rather than regional high-temperature events. That said, high temperatures in July and August in southern China enacted the precondition for heat events, and the dates of the susceptible growth-stage eventually determined the final period of exposure to concurrent events. For example, the single-rice transplanting date was 30 days earlier (day of the year, DOY 174-198) in the upstream than in the lower Yangtze River basin (DOY 207-232). When the single-rice in Chongqing entered the grain-filling stage, rice in the middle and lower reaches of the Yangtze River just entered the jointing-booting stage. Consequently, concurrent heat-drought events had a higher frequency in the later growth-stage in the upstream than in the downstream.

Similarly, the late-rice heading date was 20 days earlier in the northern part of study area (DOY 255 in Hubei, Hunan, Anhui and Zhejiang) than in the southern part (DOY 273 in Guangdong, Guangxi and Hainan). In October, the late-rice in the northern part was mostly in the grain filling stage, whereas in the southern region, due to later planting dates, it was mostly in the

https://doi.org/10.5194/egusphere-2025-1393
Preprint. Discussion started: 4 April 2025

heading-flowering stage. Consequently, southern late rice is more susceptible to the impact of chilly and rainy conditions caused by the southward movement of cold air from the north, which converges with warm and moist air currents in the south, leading to low-temperature and continuous rainy days. This finding further emphasized the importance of using growth-stage-specific thresholds, which allowed the exact spatiotemporal overlap of climate extremes and susceptible growth stages to be captured.

4.2 The predominance of individual stress in driving concurrent events varies across different growth stages

Path analysis identified the relative contribution of individual stress to compound severity and found large differences by growth stage. For instance, individual heat stress had a larger direct effect than drought stress on H1D1 and H2D2 of single-rice, but the result was not apparent in H3D3. For concurrent chilling-rainy events of late-rice, the effects of chilling and rainy stress were comparable, with a slightly larger effect of chilling in C2R2 and a larger effect of rainy in C3R3.

Previous studies on the factors driving changes in climate extremes have reported divergent results. For example, Zhang (Zhang et al., 2022b) suggested that temperature is the dominant factor influencing compound drought and heatwave events. In contrast, Bevacqua (Bevacqua et al., 2022) speculated that precipitation trends are believed to determine the future occurrence of concurrent heat-drought events. This is because future local warming would be sufficiently large that future droughts would always coincide with moderate heat extremes, and consequently, the changes in drought frequency would become the modulating factor. Our findings revealed that drought stress exhibited widespread spatial coverage and higher severity, particularly in the middle-lower Yangtze River Basin, where concurrent heat-drought events mostly occurred, particularly during the jointing-booting (H1D1) and heading-flowering (H2D2) stages (Fig. A1d, e). The heat stress demonstrated spatially concentrated patterns with a limited spatial extent (Fig. A1a, b). This spatial dichotomy highlights the fact that heat stress emerges as the dominant driver of concurrent heat-drought events, where its localized intensification, superimposed on drought conditions, triggers compound cascading effects. However, heat stress in growth stage#3 in the Sichuan and Chongqing regions was slightly more severe than that in drought. (Fig. A1 c, f), thus, the heat in this region has a slightly higher impact on the occurrence events.

The results of the path analysis showed a correlation between the heat stress and drought stress of the concurrent heat-drought event (Fig. 4c, DC_{co}). Previous studies have shown that enhanced dry-hot dependence can lead to more frequent concurrent heat-drought events (Hao and Singh, 2020; Zscheischler and Seneviratne, 2017). The combination of these processes leads to a strong negative temperature-soil moisture correlation, which can be explained by two pathways: land-atmosphere feedbacks and weather-scale correspondence between clouds and incoming shortwave radiation. Specifically, soil moisture deficits caused by low precipitation can lead to reduced evaporative cooling, along with increased sensible heat fluxes and higher surface air temperatures. High-temperature anomalies accelerate evapotranspiration, which further depletes soil moisture (Liu et al., 2020; Miralles et al., 2019). In addition, low levels of cloudiness associated with low precipitation (and subsequent soil

https://doi.org/10.5194/egusphere-2025-1393
Preprint. Discussion started: 4 April 2025

moisture deficits) tend to enhance incoming shortwave radiation, which leads to higher surface air temperatures (Berg et al., 2015). For chilling-rainy events for late-rice, our results also indicated a weak individual chilling and rainy correlation (Fig. 4d, DC_{co}). However, compared with heat-drought events, the relationships behind chilling-rainy events have largely been ignored in previous studies, and the underlying mechanism requires further investigation (Trotsiuk et al., 2020).

4.3 The sensitivity and impact of yield reduction to concurrent events differed by growth stages

Our study evaluated the historical yield impact and yield sensitivity of concurrent climate extremes across different sensitive growth stages and found comparable yield losses from concurrent heat-drought and chilling-rainy events (Fig. 5a-e). Yield sensitivity also exhibited comparable values between heat-drought events (0.29 on average) and chilling-rainy events (0.19–0.37). This comparable effect is due to the disruption of physiological processes, such as photosynthesis and nutrient uptake, while increasing pest and disease risks caused by chilling or excessive rainfall (Arshad et al., 2017; Fu et al., 2023; Jiang et al., 2010). Therefore, results add important evidence about the yield impact of compound chilling-rainy for rice, to those that have reported heat-drought events on crops such as maize and soybeans (Luan et al., 2021; Seneviratne et al., 2010).

Our results also revealed significantly different historical yield impacts across growth stages, particularly for heat-drought events (Fig. 5f). These differences in historical yield reductions likely stem from the interplay between exposed regions, regional climate couplings, and local infrastructure. Variations in regional climatic conditions drive differential responses of rice yields to extreme events across geographical areas (Li and Tao, 2023). The concentration of H3D3 events in the Sichuan-Chongqing hotspot was amplified by topography-driven vapor pressure deficit anomalies (Zhu et al., 2024), which intensified moisture stress and ultimately led to severe yield losses in this region. Additionally, the Sichuan-Chongqing region is a hilly area with difficulty in providing irrigation infrastructure (Ye et al., 2012), and crop cultivation here heavily relies on precipitation. Therefore, a lack of irrigation infrastructure can exacerbate yield losses under persistent hot and drought conditions(Hao et al., 2023).

Rice sensitivity to compound events also differed substantially according to the growth stage. Specifically, single-rice showed the highest sensitivity to heat-drought events during the grain filling stage, followed by the heading-flowering and jointing-booting stage. Late-rice exhibited greater sensitivity during the heading-flowering stage than during the grain filling stage. These growth-stage-specific patterns may be attributed to the physiological vulnerabilities of rice at different growth stages and the mechanisms by which climatic stressors exert their effects. Although experimental studies explicitly revealing the mechanisms of yield reduction under compound events remain limited, plausible explanations can be inferred from the physiological responses of rice to individual stressors. For instance, heat stress during the grain filling process inhibits the grain starch biosynthesis and shortens the grain filling duration, leading to reduced grain weight and yield (Cao et al., 2008; Tenorio et al., 2013). Drought negatively impacts photosynthetic rate and chlorophyll content, while drought occurring during the grain filling stage reduces the 1000-grain weight, ultimately leading to yield loss (Amin et al., 2022). Chilling stress during

https://doi.org/10.5194/egusphere-2025-1393
Preprint. Discussion started: 4 April 2025

the heading-flowering stage impairs rice yield by inhibiting spikelet opening, inducing spikelet sterility, and potentially leading to spikelet abortion and incomplete panicle exertion (Arshad et al., 2017; Suh et al., 2010). Rainy stress exerts a physical disturbance on pollination, thereby reducing the number of filled grains per panicle. Additionally, the overcast conditions associated with rainy stress severely impair photosynthetic assimilation in rice (Luo et al., 2018; Proctor, 2023).

4.4 Limitations

Our study was limited by the length of the time-series of data. Agrometeorological station data were only available up to 2018, and recent years that had experienced the most pronounced warming (IPCC, 2021) were therefore not included in the analysis. In particular, the severe concurrent heat-drought event in southern China in 2022 had a substantial impact on rice production (Hao et al., 2023). The absence of above data might have led to underestimates of the temporal trend and yield impact. We focused on concurrent climate extremes only in this research. However, climate extremes can occur consecutively in different growth stages (Zscheischler et al., 2020). Several studies have discussed the yield impact of switches of dry-and-wet in different stages of rice growth (Chen and Wang, 2023). Due to limited sample size, other types of compound climate extremes (like consecutive climate extremes, where rice is impacted by one event at one growth-stage, and by another at a different growth-stage) were not discussed in this study, but requires future investigation, including its spatial temporal variation, possible physical compound mechanisms, and the underlying process of yield loss.

5 Conclusions

In this study, we investigated the spatiotemporal variation of concurrent compound extremes for single- and late-rice in southern China and their underlying climate drivers, by distinguishing growth-stage-specific event types and thresholds. Temporally, our results indicated a significant increasing trend of concurrent heat-drought events for single-rice and a slight increasing trend for concurrent chilling-rainy events for late-rice. Spatially, the hotspots of concurrent heat-drought events for single-rice shifted from the lower Yangtze River Basin to its upper stream, and were dominated by the spatial differences in phenology rather than the occurrence of extreme events. The concurrent chilling-rainy events of late-rice were widespread within the planting regions, with a higher incidence at higher altitudes and latitudes. Path analysis suggested that heat stress had a larger direct effect than drought on compound severity, particularly in H1D1 and H2D2. For concurrent chilling-rainy events of late-rice, the effects of chilling and rainy stress were comparable. The assessment of compound event impacts and sensitivity to rice yield revealed significant growth-stage-specific differences, with comparable yield losses from both concurrent heat-drought and chilling-rainy events.

Recent studies have provided additional details regarding the impacts of compound events on other staple crops (Hamed et al., 2021), or single climate extremes for rice (Fu et al., 2023). A straightforward extension of the present study was to project the future occurrence and severity of compound extremes for rice. It is also important to project future yield impacts of compound

https://doi.org/10.5194/egusphere-2025-1393
Preprint. Discussion started: 4 April 2025

extreme events for rice, for risk management and adaptation purposes. Such a projection requires quantitative vulnerability functions or growth model simulations of compound extreme events. To increase the capability of the models, controlled experiments and field observations are needed to improve our understanding of the imapcat of compound extremes on rice (Lesk et al., 2022). Consequently, our study provides critical insights into the comprehensive impacts of compound events on rice production and establishes a scientific foundation for developing targeted adaptation strategies.

https://doi.org/10.5194/egusphere-2025-1393
Preprint. Discussion started: 4 April 2025

Appendix A: Additional Figures

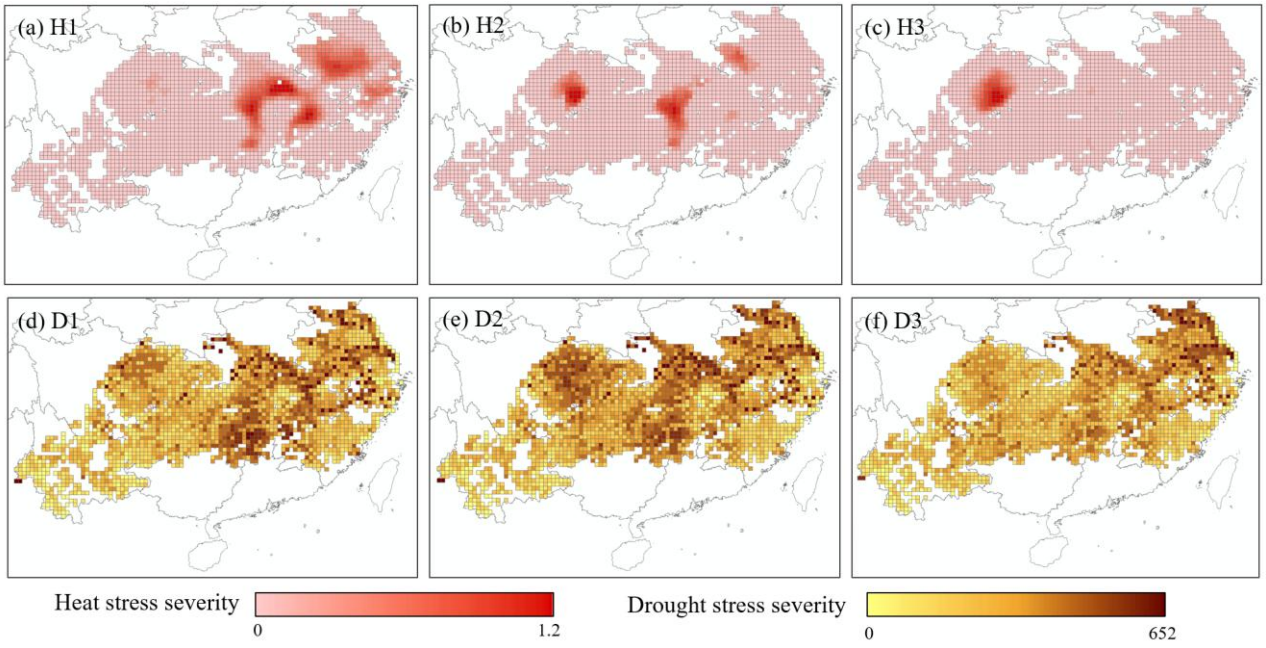

Figure A1. Spatial distribution of single heat and drought extreme events of rice for the period of 1981-2018. Each subgraph represents the frequency of (a-c) heat events, (d-f) drought events.

Author contributions

Tao Ye designed the research. Material preparation, data collection and analysis were performed by Ran Sun, Yiqing Liu, Weihang Liu and Shuo Chen. Ran Sun darfted the manuscript and Tao Ye revised it. All authors commented on previous versions of the manuscript. All authors read and approved the final manuscript.

Data availability

Rice phenology data recorded by agrometeorological stations are available through the China Meteorological Administration (CMA) at http://data.cma.cn. The daily meteorological dataset of basic meteorological elements of China National Surface Weather Station (V3.0) are also available through the China Meteorological Administration (CMA) at http://data.cma.cn. The 0.25° gridded daily 0-10 cm soil moisture data are available through the surface hydrology dataset VIC-CN05.1 at https://doi.org/10.1016/j.jhydrol.2020.125413 (Miao and Wang, 2020).

Code availability

The code is available from the corresponding author upon reasonable request.

https://doi.org/10.5194/egusphere-2025-1393
Preprint. Discussion started: 4 April 2025

Competing interests

The authors have no relevant financial or non-financial interests to disclose.

Acknowledgments

This study has been financially supported by National Natural Science Foundation of China (NSFC. 42171075), and the project jointly funded by National Natural Science Foundation of China (NSFC. 72261147759) and the Bill & Melinda Gates Foundation (2022YFAG1004).

AI tools were used for sentence and format checking.

References

Amin, M. W., Aryan, S., Habibi, N., Kakar, K., and Zahid, T.: Elucidation of photosynthesis and yield performance of rice (Oryza sativa L.) under drought stress conditions, Plant Physiol. Rep., 27, 143–151, https://doi.org/10.1007/s40502-021-00613-0, 2022.

Arshad, M. S., Farooq, M., Asch, F., Krishna, J. S. V., Prasad, P. V. V., and Siddique, K. H. M.: Thermal stress impacts reproductive development and grain yield in rice, Plant Physiology and Biochemistry, 115, 57–72, https://doi.org/10.1016/j.plaphy.2017.03.011, 2017.

Berg, A., Lintner, B. R., Findell, K., Seneviratne, S. I., Hurk, B. van den, Ducharne, A., Chéruy, F., Hagemann, S., Lawrence, D. M., Malyshev, S., Meier, A., and Gentine, P.: Interannual Coupling between Summertime Surface Temperature and Precipitation over Land: Processes and Implications for Climate Change, Journal of Climate, 28, 1308–1328, https://doi.org/10.1175/JCLI-D-14-00324.1, 2015.

Bevacqua, E., Zappa, G., Lehner, F., and Zscheischler, J.: Precipitation trends determine future occurrences of compound hot–dry events, Nat. Clim. Chang., 12, 350–355, https://doi.org/10.1038/s41558-022-01309-5, 2022.

Cao, Y.-Y., Duan, H., Yang, L.-N., Wang, Z.-Q., Zhou, S.-C., and Yang, J.-C.: Effect of Heat Stress During Meiosis on Grain Yield of Rice Cultivars Differing in Heat Tolerance and Its Physiological Mechanism, Acta Agronomica Sinica, 34, 2134–2142, https://doi.org/10.1016/S1875-2780(09)60022-5, 2008.

Chen, H. and Wang, S.: Compound Dry and Wet Extremes Lead to an Increased Risk of Rice Yield Loss, Geophysical Research Letters, 50, e2023GL105817, https://doi.org/10.1029/2023GL105817, 2023.

Chen, J., Liu, Y., Zhou, W., Zhang, J., and Pan, T.: Effects of climate change and crop management on changes in rice phenology in China from 1981 to 2010, Journal of the Science of Food and Agriculture, 101, 6311–6319, https://doi.org/10.1002/jsfa.11300, 2021.

Chenu, K., Porter, J. R., Martre, P., Basso, B., Chapman, S. C., Ewert, F., Bindi, M., and Asseng, S.: Contribution of Crop Models to Adaptation in Wheat, Trends in Plant Science, 22, 472–490, https://doi.org/10.1016/j.tplants.2017.02.003, 2017.

https://doi.org/10.5194/egusphere-2025-1393
Preprint. Discussion started: 4 April 2025

Feng, S., Hao, Z., Wu, X., Zhang, X., and Hao, F.: A multi-index evaluation of changes in compound dry and hot events of global maize areas, Journal of Hydrology, 602, 126728, https://doi.org/10.1016/j.jhydrol.2021.126728, 2021.

Fu, J., Jian, Y., Wang, X., Li, L., Ciais, P., Zscheischler, J., Wang, Y., Tang, Y., Müller, C., Webber, H., Yang, B., Wu, Y., Wang, Q., Cui, X., Huang, W., Liu, Y., Zhao, P., Piao, S., and Zhou, F.: Extreme rainfall reduces one-twelfth of China's rice yield over the last two decades, Nat Food, 4, 416–426, https://doi.org/10.1038/s43016-023-00753-6, 2023.

Fu, K., Yu, H., Zhang, Y., Zhu, D., Liu, H., and Wang, K.: Flash drought and heatwave compound events increased in strength and length from 1980 to 2022 in China, Weather and Climate Extremes, 46, 100720, https://doi.org/10.1016/j.wace.2024.100720, 2024.

Guo, C., Ren, J., Wang, D., Cui, J., Mu, J., Liu, W., and Cao, T.: Temporal and Spatial Characteristics of Rice Cold Damage in Jilin from 1961 to 2018, Chinese Agricultural Science Bulletin, 36, 109, https://doi.org/10.11924/j.issn.1000-6850.casb20191000766, 2020.

Hamed, R., Van Loon, A. F., Aerts, J., and Coumou, D.: Impacts of compound hot–dry extremes on US soybean yields, Earth Syst. Dynam., 12, 1371–1391, https://doi.org/10.5194/esd-12-1371-2021, 2021.

Hao, Z. and Singh, V. P.: Compound Events under Global Warming: A Dependence Perspective, Journal of Hydrologic Engineering, 25, 03120001, https://doi.org/10.1061/(ASCE)HE.1943-5584.0001991, 2020.

Hao, Z., Chen, Y., Feng, S., Liao, Z., An, N., and Li, P.: The 2022 Sichuan-Chongqing spatio-temporally compound extremes: a bitter taste of novel hazards, Science Bulletin, 68, 1337–1339, https://doi.org/10.1016/j.scib.2023.05.034, 2023.

Haqiqi, I., Grogan, D. S., Hertel, T. W., and Schlenker, W.: Quantifying the impacts of compound extremes on agriculture, Hydrology and Earth System Sciences, 25, 551–564, https://doi.org/10.5194/hess-25-551-2021, 2021.

He, Y., Hu, X., Xu, W., Fang, J., and Shi, P.: Increased probability and severity of compound dry and hot growing seasons over world's major croplands, Science of The Total Environment, 824, 153885, https://doi.org/10.1016/j.scitotenv.2022.153885, 2022.

Jiang, W., Lee, J., Chu, S.-H., Ham, T.-H., Woo, M.-O., Cho, Y.-I., Chin, J.-H., Han, L., Xuan, Y., Yuan, D., Xu, F., Dai, L., Yea, J.-D., and Koh, H.-J.: Genotype × environment interactions for chilling tolerance of rice recombinant inbred lines under different low temperature environments, Field Crops Research, 117, 226–236, https://doi.org/10.1016/j.fcr.2010.03.007, 2010.

IPCC: IPCC, 2021: Climate Change 2021: The Physical Science Basis. Contribution of Working Group I to the Sixth Assessment Report of the Intergovernmental Panel on Climate Change, Cambridge University Press, Cambridge, United Kingdom and New York, NY, USA, https://doi.org/10.1017/9781009157896, 2021.

IPCC: IPCC 2022: Climate Change 2022: Impacts, Adaptation and Vulnerability | Climate Change 2022: Impacts, Adaptation and Vulnerability, 2022.

Kern, A., Barcza, Z., Marjanović, H., Árendás, T., Fodor, N., Bónis, P., Bognár, P., and Lichtenberger, J.: Statistical modelling of crop yield in Central Europe using climate data and remote sensing vegetation indices, Agricultural and Forest Meteorology, 260–261, 300–320, https://doi.org/10.1016/j.agrformet.2018.06.009, 2018.

https://doi.org/10.5194/egusphere-2025-1393
Preprint. Discussion started: 4 April 2025

Lesk, C. and Anderson, W.: Decadal variability modulates trends in concurrent heat and drought over global croplands, Environ. Res. Lett., 16, 055024, https://doi.org/10.1088/1748-9326/abeb35, 2021.

Lesk, C., Coffel, E., Winter, J., Ray, D., Zscheischler, J., Seneviratne, S. I., and Horton, R.: Stronger temperature–moisture couplings exacerbate the impact of climate warming on global crop yields, Nat Food, 2, 683–691, https://doi.org/10.1038/s43016-021-00341-6, 2021.

Lesk, C., Anderson, W., Rigden, A., Coast, O., Jägermeyr, J., McDermid, S., Davis, K. F., and Konar, M.: Compound heat and moisture extreme impacts on global crop yields under climate change, Nat Rev Earth Environ, 3, 872–889, https://doi.org/10.1038/s43017-022-00368-8, 2022.

Li, H. W., Li, Y. P., Huang, G. H., and Sun, J.: Quantifying effects of compound dry-hot extremes on vegetation in Xinjiang (China) using a vine-copula conditional probability model, Agricultural and Forest Meteorology, 311, 108658, https://doi.org/10.1016/j.agrformet.2021.108658, 2021.

Li, Y. and Tao, F.: Rice yield response to climate variability diverges strongly among climate zones across China and is sensitive to trait variation, Field Crops Research, 301, 109034, https://doi.org/10.1016/j.fcr.2023.109034, 2023.

Li, Z., Liu, W., Ye, T., Chen, S., and Shan, H.: Observed and CMIP6 simulated occurrence and intensity of compound agroclimatic extremes over maize harvested areas in China, Weather and Climate Extremes, 38, 100503, https://doi.org/10.1016/j.wace.2022.100503, 2022.

Liu, X., Zhang, Z., Shuai, J., Wang, P., Shi, W., Tao, F., and Chen, Y.: Impact of chilling injury and global warming on rice yield in Heilongjiang Province, J. Geogr. Sci., 23, 85–97, https://doi.org/10.1007/s11442-013-0995-9, 2013.

Liu, X., He, B., Guo, L., Huang, L., and Chen, D.: Similarities and Differences in the Mechanisms Causing the European Summer Heatwaves in 2003, 2010, and 2018, Earth's Future, 8, e2019EF001386, https://doi.org/10.1029/2019EF001386, 2020.

Liu, Y., Liu, W., Li, Y., Ye, T., Chen, S., Li, Z., and Sun, R.: Concurrent Precipitation Extremes Modulate the Response of Rice Transplanting Date to Preseason Temperature Extremes in China, Earth's Future, 11, e2022EF002888, https://doi.org/10.1029/2022EF002888, 2023.

Lobell, D. B. and Gourdji, S. M.: The Influence of Climate Change on Global Crop Productivity, Plant Physiology, 160, 1686–1697, https://doi.org/10.1104/pp.112.208298, 2012.

Lu, Y., Hu, H., Li, C., and Tian, F.: Increasing compound events of extreme hot and dry days during growing seasons of wheat and maize in China, Sci Rep, 8, 16700, https://doi.org/10.1038/s41598-018-34215-y, 2018.

Luan, X., Bommarco, R., Scaini, A., and Vico, G.: Combined heat and drought suppress rainfed maize and soybean yields and modify irrigation benefits in the USA, Environ. Res. Lett., 16, 064023, https://doi.org/10.1088/1748-9326/abfc76, 2021.

Luo, K., Zeng, Y., Hu, Q., Chen, L., Yi, Y., Sui, F., and Li, X.: Effects of Weak Light Stress at Different Stages on Sink-source Characteristics and Protective Enzyme Activities in Leaf of Late Rice Varieties with Different Tolerance, Chinese Journal OF Rice Science, 32, 581, https://doi.org/10.16819/j.1001-7216.2018.7146, 2018.

https://doi.org/10.5194/egusphere-2025-1393
Preprint. Discussion started: 4 April 2025

Luo, Y., Zhang, Z., Chen, Y., Li, Z., and Tao, F.: ChinaCropPhen1km: a high-resolution crop phenological dataset for three staple crops in China during 2000–2015 based on leaf area index (LAI) products, Earth System Science Data, 12, 197–214, https://doi.org/10.5194/essd-12-197-2020, 2020.

Madadgar, S., AghaKouchak, A., Shukla, S., Wood, A. W., Cheng, L., Hsu, K.-L., and Svoboda, M.: A hybrid statistical-dynamical framework for meteorological drought prediction: Application to the southwestern United States, Water Resources Research, 52, 5095–5110, https://doi.org/10.1002/2015WR018547, 2016.

Mazdiyasni, O., Sadegh, M., Chiang, F., and AghaKouchak, A.: Heat wave Intensity Duration Frequency Curve: A Multivariate Approach for Hazard and Attribution Analysis, Sci Rep, 9, 14117, https://doi.org/10.1038/s41598-019-50643-w, 2019.

Miao, Y. and Wang, A.: A daily 0.25° × 0.25° hydrologically based land surface flux dataset for conterminous China, 1961–2017, Journal of Hydrology, 590, 125413, https://doi.org/10.1016/j.jhydrol.2020.125413, 2020.

Miralles, D. G., Gentine, P., Seneviratne, S. I., and Teuling, A. J.: Land–atmospheric feedbacks during droughts and heatwaves: state of the science and current challenges, Annals of the New York Academy of Sciences, 1436, 19–35, https://doi.org/10.1111/nyas.13912, 2019.

Pan, B., Zheng, Y., Shen, R., Ye, T., Zhao, W., Dong, J., Ma, H., and Yuan, W.: High Resolution Distribution Dataset of Double-Season Paddy Rice in China, Remote Sensing, 13, 4609, https://doi.org/10.3390/rs13224609, 2021.

Proctor, J.: Extreme rainfall reduces rice yields in China, Nat Food, 4, 360–361, https://doi.org/10.1038/s43016-023-00757-2, 2023.

Ribeiro, A. F. S., Russo, A., Gouveia, C. M., Páscoa, P., and Zscheischler, J.: Risk of crop failure due to compound dry and hot extremes estimated with nested copulas, Biogeosciences, 17, 4815–4830, https://doi.org/10.5194/bg-17-4815-2020, 2020.

Rötter, R. P., Appiah, M., Fichtler, E., Kersebaum, K. C., Trnka, M., and Hoffmann, M. P.: Linking modelling and experimentation to better capture crop impacts of agroclimatic extremes—A review, Field Crops Research, 221, 142–156, https://doi.org/10.1016/j.fcr.2018.02.023, 2018.

Sadegh, M., Moftakhari, H., Gupta, H. V., Ragno, E., Mazdiyasni, O., Sanders, B., Matthew, R., and AghaKouchak, A.: Multihazard Scenarios for Analysis of Compound Extreme Events, Geophysical Research Letters, 45, 5470–5480, https://doi.org/10.1029/2018GL077317, 2018.

Salvadori, G., Durante, F., De Michele, C., Bernardi, M., and Petrella, L.: A multivariate copula-based framework for dealing with hazard scenarios and failure probabilities, Water Resources Research, 52, 3701–3721, https://doi.org/10.1002/2015WR017225, 2016.

Sehgal, A., Sita, K., Siddique, K. H. M., Kumar, R., Bhogireddy, S., Varshney, R. K., HanumanthaRao, B., Nair, R. M., Prasad, P. V. V., and Nayyar, H.: Drought or/and Heat-Stress Effects on Seed Filling in Food Crops: Impacts on Functional Biochemistry, Seed Yields, and Nutritional Quality, Front Plant Sci, 9, 1705, https://doi.org/10.3389/fpls.2018.01705, 2018.

https://doi.org/10.5194/egusphere-2025-1393
Preprint. Discussion started: 4 April 2025

Seneviratne, S. I., Corti, T., Davin, E. L., Hirschi, M., Jaeger, E. B., Lehner, I., Orlowsky, B., and Teuling, A. J.: Investigating soil moisture–climate interactions in a changing climate: A review, Earth-Science Reviews, 99, 125–161, https://doi.org/10.1016/j.earscirev.2010.02.004, 2010.

Shen, R., Pan, B., Peng, Q., Dong, J., Chen, X., Zhang, X., Ye, T., Huang, J., and Yuan, W.: High-resolution distribution maps of single-season rice in China from 2017 to 2022, Earth System Science Data, 15, 3203–3222, https://doi.org/10.5194/essd-15-3203-2023, 2023.

Suh, J. P., Jeung, J. U., Lee, J. I., Choi, Y. H., Yea, J. D., Virk, P. S., Mackill, D. J., and Jena, K. K.: Identification and analysis of QTLs controlling cold tolerance at the reproductive stage and validation of effective QTLs in cold-tolerant genotypes of rice (Oryza sativa L.), Theor Appl Genet, 120, 985–995, https://doi.org/10.1007/s00122-009-1226-8, 2010.

Tan, S., Fan, J., Yan, S., Tao, X., Ou, J., and Luo, H.: Meteorological Disasters at Long-term Scales: Influence on Rice Yield of Hunan, Chinese Agricultural Science Bulletin, 36, 104, https://doi.org/10.11924/j.issn.1000-6850.casb20190400005, 2020.

Tavakol, A., Rahmani, V., and Jr, J. H.: Probability of compound climate extremes in a changing climate: A copula-based study of hot, dry, and windy events in the central United States, Environ. Res. Lett., 2020.

Tenorio, F. A., Ye, C., Redona, E., Sierra, S., Laza, M., and Argayoso, M.: Screening rice genetic resource for heat tolerance, SABRAO Journal of Breeding and Genetics, 45, 341–351, 2013.

Trnka, M., Rötter, R. P., Ruiz-Ramos, M., Kersebaum, K. C., Olesen, J. E., Žalud, Z., and Semenov, M. A.: Adverse weather conditions for European wheat production will become more frequent with climate change, Nature Clim Change, 4, 637–643, https://doi.org/10.1038/nclimate2242, 2014.

Trotsiuk, V., Hartig, F., Cailleret, M., Babst, F., Forrester, D. I., Baltensweiler, A., Buchmann, N., Bugmann, H., Gessler, A., Gharun, M., Minunno, F., Rigling, A., Rohner, B., Stillhard, J., Thürig, E., Waldner, P., Ferretti, M., Eugster, W., and Schaub, M.: Assessing the response of forest productivity to climate extremes in Switzerland using model–data fusion, Global Change Biology, 26, 2463–2476, https://doi.org/10.1111/gcb.15011, 2020.

Urban, O., Hlaváčová, M., Klem, K., Novotná, K., Rapantová, B., Smutná, P., Horáková, V., Hlavinka, P., Škarpa, P., and Trnka, M.: Combined effects of drought and high temperature on photosynthetic characteristics in four winter wheat genotypes, Field Crops Research, 223, 137–149, https://doi.org/10.1016/j.fcr.2018.02.029, 2018.

Vandenberghe, S., Verhoest, N. E. C., and De Baets, B.: Fitting bivariate copulas to the dependence structure between storm characteristics: A detailed analysis based on 105 year 10 min rainfall, Water Resources Research, 46, https://doi.org/10.1029/2009WR007857, 2010.

Wang, L., Liao, S., Huang, S., Ming, B., Meng, Q., and Wang, P.: Increasing concurrent drought and heat during the summer maize season in Huang–Huai–Hai Plain, China, Intl Journal of Climatology, 38, 3177–3190, https://doi.org/10.1002/joc.5492, 2018.

https://doi.org/10.5194/egusphere-2025-1393
Preprint. Discussion started: 4 April 2025

Wu, H., Zhang, J., Zhang, Z., Han, J., Cao, J., Zhang, L., Luo, Y., Mei, Q., Xu, J., and Tao, F.: AsiaRiceYield4km: seasonal rice yield in Asia from 1995 to 2015, Earth System Science Data, 15, 791–808, https://doi.org/10.5194/essd-15-791-2023, 2023.

Wu J. and Gao X.: A gridded daily observation dataset over China region and comparison with the other datasets, Chinese Journal of Geophysics, 56, 1102–1111, https://doi.org/10.6038/cjg20130406, 2013.

Xie, Y., Huang, S., Tian, J., Wang, Y., and Ye, Q.: Spatial-temporal characteristics of thermal resources and its influence on the growth of double cropping rice in the middle and lower reaches of the Yangtze River,China., Chinese Journal of Applied Ecology, 27, 2950, https://doi.org/10.13287/j.1001-9332.201609.013, 2016.

Xiong, W., Feng, L., Ju, H., and Yang, D.: Possible Impacts of High Temperatures on China's Rice Yield under Climate Change, Advances in Earth Science, 31, 515, https://doi.org/10.11867/j.issn.1001-8166.2016.05.0515, 2016.

Ye, T., Shi, P., Wang, J., Liu, L., Fan, Y., and Hu, J.: China's drought disaster risk management: Perspective of severe droughts in 2009–2010, Int J Disaster Risk Sci, 3, 84–97, https://doi.org/10.1007/s13753-012-0009-z, 2012.

Ye, T., Nie, J., Wang, J., Shi, P., and Wang, Z.: Performance of detrending models of crop yield risk assessment: evaluation on real and hypothetical yield data, Stoch Environ Res Risk Assess, 29, 109–117, https://doi.org/10.1007/s00477-014-0871-x, 2015.

Yu, R., Dong, S., Han, Z., and Li, W.: Increased exposure of rice to compound drought and hot extreme events during its growing seasons in China, Ecological Indicators, 167, 112735, https://doi.org/10.1016/j.ecolind.2024.112735, 2024.

Zhang, L., Guo, A., He, L., Hou, Y., Zhao, X., Qian, Y., and Cai, Z.: Variation Characteristics of Chilling Dew Wind for Double-Season Late Rice Across Southern China in 2020, Meteorological Monthly, 47, 1537–1545, https://doi.org/10.7519/j.issn.1000-0526.2021.12.009, 2021.

Zhang, L., Zhang, Z., Tao, F., Luo, Y., Zhang, J., and Cao, J.: Adapting to climate change precisely through cultivars renewal for rice production across China: When, where, and what cultivars will be required?, Agricultural and Forest Meteorology, 316, 108856, https://doi.org/10.1016/j.agrformet.2022.108856, 2022a.

Zhang, Q., She, D., Zhang, L., Wang, G., Chen, J., and Hao, Z.: High Sensitivity of Compound Drought and Heatwave Events to Global Warming in the Future, Earth's Future, 10, e2022EF002833, https://doi.org/10.1029/2022EF002833, 2022b.

Zhang, Y., Hao, Z., Feng, S., Zhang, X., and Hao, F.: Changes and driving factors of compound agricultural droughts and hot events in eastern China, Agricultural Water Management, 263, 107485, https://doi.org/10.1016/j.agwat.2022.107485, 2022c.

Zhang, Z., Wang, P., Chen, Y., Song, X., Wei, X., and Shi, P.: Global warming over 1960–2009 did increase heat stress and reduce cold stress in the major rice-planting areas across China, European Journal of Agronomy, 59, 49–56, https://doi.org/10.1016/j.eja.2014.05.008, 2014.

Zhao, H., Fu, Y. H., Wang, X., Zhao, C., Zeng, Z., and Piao, S.: Timing of rice maturity in China is affected more by transplanting date than by climate change, Agricultural and Forest Meteorology, 216, 215–220, https://doi.org/10.1016/j.agrformet.2015.11.001, 2016.

https://doi.org/10.5194/egusphere-2025-1393
Preprint. Discussion started: 4 April 2025

Zhu, Y. and Yang, S.: Evaluation of CMIP6 for historical temperature and precipitation over the Tibetan Plateau and its comparison with CMIP5, Advances in Climate Change Research, 11, 239–251, https://doi.org/10.1016/j.accre.2020.08.001, 2020.

Zhu, Y., Li, Y., Zhou, X., Feng, W., Gao, G., Li, M., and Zheng, G.: Causes of the severe drought in Southwest China during the summer of 2022, Atmospheric Research, 303, 107320, https://doi.org/10.1016/j.atmosres.2024.107320, 2024.

Zscheischler, J. and Seneviratne, S. I.: Dependence of drivers affects risks associated with compound events, Sci. Adv., 3, e1700263, https://doi.org/10.1126/sciadv.1700263, 2017.

Zscheischler, J., Martius, O., Westra, S., Bevacqua, E., Raymond, C., Horton, R. M., van den Hurk, B., AghaKouchak, A., Jézéquel, A., Mahecha, M. D., Maraun, D., Ramos, A. M., Ridder, N. N., Thiery, W., and Vignotto, E.: A typology of compound weather and climate events, Nat Rev Earth Environ, 1, 333–347, https://doi.org/10.1038/s43017-020-0060-z, 2020.